Received: 17 January 2018 | Revised: 11 May 2018 | Accepted: 14 May 2018

DOI: 10.1002/mrm.27392

NOTE

Magnetic Resonance in Medicine

Independent validation of metric optimized gating for fetal cardiovascular phase-contrast flow imaging

Sebastian Bidhult[1,2] | **Johannes Töger**[1] | **Einar Heiberg**[1,2] | **Marcus Carlsson**[1] | **Håkan Arheden**[1] | **Anthony H. Aletras**[1,3] | **Erik Hedström**[1,4]

[1]Lund University, Skane University Hospital, Department of Clinical Sciences Lund, Clinical Physiology, Lund, Sweden

[2]Lund University, Department of Biomedical Engineering, Faculty of Engineering, Lund, Sweden

[3]Laboratory of Computing, Medical Informatics and Biomedical–Imaging Technologies, School of Medicine, Aristotle University of Thessaloniki, Greece

[4]Lund University, Skane University Hospital, Department of Clinical Sciences Lund, Diagnostic Radiology, Lund, Sweden

Correspondence
Erik Hedström, Department of Clinical Sciences Lund, Lund University, SE-221 00, Lund, Sweden. Email: erik.hedstrom@med.lu.se

Funding information
Swedish Heart and Lung Foundation, Grant/Award Number: 20160554; Swedish Research Council; Medical Faculty at Lund University; Region of Skåne, and the Greek General Secretariat for Research and Development via an Excellence grant; Medical Faculty at Lund University, and Region of Skåne; Greek General Secretariat for Research and Development via an Excellence grant; Vetenskapsrådet, Grant/Award Number: 2016-01617.

Purpose: To validate metric optimized gating phase-contrast MR (MOG PC-MR) flow measurements for a range of fetal flow velocities in phantom experiments. 2) To investigate intra- and interobserver variability for fetal flow measurements at an imaging center other than the original site.

Methods: MOG PC-MR was compared to timer/beaker measurements in a pulsatile flow phantom using a heart rate (~145 bpm), nozzle diameter (~6 mm), and flow range (~130–700 mL/min) similar to fetal imaging. Fifteen healthy fetuses were included for intra- and interobserver variability in the fetal descending aorta and umbilical vein.

Results: Phantom MOG PC-MR flow bias and variability was 2% ± 23%. Accuracy of MOG PC-MR was degraded for flow profiles with low velocity-to-noise ratio. Intra- and interobserver coefficients of variation were 6% and 19%, respectively, for fetal descending aorta; and 10% and 17%, respectively, for the umbilical vein.

Conclusion: Phantom validation showed good agreement between MOG and conventionally gated PC-MR, except for cases with low velocity-to-noise ratio, which resulted in MOG misgating and underestimated peak velocities and warranted optimization of sequence parameters to individual fetal vessels. Inter- and intraobserver variability for fetal MOG PC-MR imaging were comparable to previously reported values.

KEYWORDS
fetal MRI, metric optimized gating, PC-MR validation

1 | INTRODUCTION

Noninvasive measurement of blood flow in the fetal cardiovascular system may increase our knowledge of fetal cardiovascular physiology and aid in the diagnosis of diseases such as congenital heart disease and intrauterine growth restriction. Currently, the most commonly applied method for fetal blood flow measurements is pulsed Doppler ultrasound.[1,2] The technique is widely available, safe, relatively inexpensive, and has demonstrated fair reproducibility.[3] Despite numerous advantages, flow measurements by pulsed Doppler ultrasound have inherent limitations, including sensitivity to the angle between the Doppler beam and the blood flow direction, and assumptions of vessel shape and velocity profile shape across the vessel lumen are required.[4]

MRI, a nonionizing imaging modality considered safe for fetal applications,[5–9] is a viable alternative for noninvasive flow quantification by utilizing phase contrast MR (PC-MR), which has been validated extensively in large vessels[10–15] and to some extent in small vessels,[16–19] including validation in coronary vessels and phantoms similar in size to the fetal aorta and umbilical vein.[19,20] Lack of a usable electrocardiogram by surface electrodes for fetal imaging makes fetal blood flow measurements by PC-MR particularly challenging.

To overcome the need for a fetal electrocardiogram, Jansz et al. introduced metric optimized gating (MOG),[21] which has demonstrated reproducibility at 1.5T and 3T[22] and low interobserver variability for fetal applications[23,24]; however, validation and variability results published are from a single research center. Validation at multiple sites is crucial for wider application. Further, phantom validation of MOG PC-MR has not been performed for a range of flow velocities, and sensitivity to varying signal conditions is unclear. We hypothesized that the accuracy of velocity profiles from MOG PC-MR is more sensitive to varying signal conditions than conventionally gated PC-MR.

Therefore, the aims were to 1) validate MOG PC-MR flow measurements for a range of fetal flow velocities using an independent reference standard in phantom experiments; and 2) investigate intra- and interobserver variability for fetal flow measurements at an additional imaging center.

2 | METHODS

The study was approved by the regional ethical review board in Lund, Sweden, and complies with the Declaration of Helsinki. Written informed consent was obtained from all study subjects, and MR imaging was performed at a 1.5T scanner (Aera, Siemens Healthcare, Erlangen, Germany) using one 16-channel phased-array chest coil and 1 spine imaging coil. Image processing and measurements, except for MOG reconstruction, were performed using the medical image analysis software Segment v2.0 (Medviso AB, Lund Sweden).[25]

TABLE 1 MRI sequence parameters in use

MRI Sequence Parameters	Phantom Imaging MOG PC-MR	Phantom Imaging Gated PC-MR Matched	Phantom Imaging Gated PC-MR Velocity Reference Standard	Phantom Imaging 3D-bSSFP	Fetal Imaging MOG PC-MR
Flip angle (°)	20	20	20	48	20
TE/TR (ms)	2.8/5.1	2.8/5.1	3.2/5.6	3.5/7.0	2.8/5.1
VENC (cm/s)	150	150	150 or 80	NA	150
Acquired temporal resolution (ms)	30.5	30.5	11.2	NA	30.4
Acquired voxel size (mm^3)	1.3×1.3×5	1.3×1.3×5	1.0×1.0×5	0.4×0.4×0.4	1.3×1.3×5
Views per segment	3	3	1	Single shot	3
Acquisition time (s)	29	29	116	638	29

VENC, velocity encoding; bSSFP = balanced steady-state free-precession; MOG PC-MR, metric optimized gating phase-contrast MR; VNR, velocity-to-noise ratio.

2.1 | Phantom validation

Phantom experiments were performed to validate MOG PC-MR against an independent flow reference standard using a heart rate (~145 beats per minute [bpm]), a vessel diameter (~6 mm), and a flow (~130–700 mL/min) similar to fetal conditions. A pulsatile flow phantom[26] consisting of a servo motor driven pump and a flow rectifier connected to a water tank was extended with an outflow nozzle submerged in water with an inner diameter (6 mm) comparable to the umbilical vein and fetal descending aorta during the third trimester.[27,28] The pump frequency was set to 145 bpm, and a trigger signal was forwarded to the MR system for conventional image gating. 2D PC-MR images were acquired in a transversal plane perpendicular to the nozzle tube. Three gradient recalled echo PC-MR sequences were evaluated: 1 MOG PC-MR sequence (Table 1, column 2) and 2 versions of a conventionally gated PC-MR sequence (Table 1, columns 3 and 4).

The 2 conventionally gated acquisitions differed in sequence parameters in order to have 1 set of parameters similar to the MOG PC-MR sequence (Table 1, column 3; gated PC-MR matched) and 1 set of parameters with improved temporal and spatial resolution to be used as reference standard measurement for velocity (Table 1, column 4; gated PC-MR velocity reference standard). MOG PC-MR was compared to the gated PC-MR matched sequence in order to exclude differences in sequence parameter settings as a confounding factor.

Gating of the MOG PC-MR sequence was performed using a simulated electrocardiogram signal with a constant 525 ms interval between successive electrocardiogram R waves (RR-interval) in order to oversample the true RR-interval of the pump (~414 ms), as previously described.[21] MOG reconstruction was performed using the MOG-Public Software v2.7 (https://github.com/MetricOptimizedGating/MOG-Public). A square region of interest (ROI) 11 pixels wide was placed over the phantom outflow nozzle, also covering areas with stationary water, and a 2-parameter heart rate model from the original MOG publication[21] was used (see Supporting Information Text S1).

Velocity encoding was set to 150 cm/s for the MOG PC-MR sequence and the gated PC-MR matched sequence, whereas a velocity encoding of either 150 cm/s or 80 cm/s was used for the gated PC-MR velocity reference standard sequence, depending on the expected peak velocity. Timer and beaker measurements were performed as an independent flow reference standard before and after PC-MR velocity measurements to detect potential flow drifts over time.

PC-MR velocity profiles and flow were obtained from manual ROI delineation. Regions of interest from the gated PC-MR matched sequence (Table 1, column 3) were copied to MOG PC-MR images to exclude delineation variability as a confounding factor. To reduce PC-MR flow variability due to manual delineations, the phantom nozzle area was measured independently by a 3D balanced steady-state free-precession sequence at 3T for improved resolution (Table 1, column 5). PC-MR maximum–minimum velocity over the RR-interval was calculated as the difference between maximum and minimum velocity over a beat. Velocity-to-noise ratio (VNR) was calculated as peak velocities divided by the noise SD, whereas SNR was calculated as the average magnitude signal divided by the noise SD. Noise SDs were estimated in a separate PC-MR measurement with the pump turned off. To investigate the impact of erroneous gating from MOG on PC-MR velocity measurements, the MOG PC-MR dataset with the highest VNR was reconstructed with preset erroneous heart rates ranging from 128 to 164 bpm. To investigate the variation of MOG gating due to random noise, numerical experiments were performed (c.f. Supporting Information Text S2).

2.2 | Fetal imaging

Fifteen healthy fetuses (gestational weeks 30–37) were prospectively included, and imaging was performed in the maternal left lateral decubitus position. A 2D PC-MR sequence was used for flow measurements in the fetal descending aorta (DAo) and the intraabdominal umbilical vein (UV). MOG PC-MR measurements were acquired during maternal breath-holds using a simulated electrocardiogram signal as described above. Cardiotocography was performed at rest 5 min before the MRI examination in 8 subjects, showing maximum RR intervals of median 444 ms (range 413–461 ms) and resulting in oversampling of 14% to 27% for MOG PC-MR. Background phase correction was performed by subtraction of a first-order polynomial. Two independent experienced observers assessed interobserver variability. One observer repeated the measurements for intraobserver variability. Noise SDs in the UV and DAo were estimated by using a noise prescan, which was integrated in the PC-MR acquisition with a previously validated algorithm.[29]

2.3 | Statistical analysis

Bias and variability of PC-MR measurements were determined using modified Bland-Altman analysis[30] with error percentages calculated as differences between 2 measurements divided by the reference standard measurement. Coefficient of variation for intra- and interobserver variability were computed as the sample SD of differences between measurements divided by their sample mean.

3 | RESULTS

3.1 | Phantom validation

Timer and beaker flow measurements ranged between 127 to 701 mL/min. The maximum difference in timer and beaker

TABLE 2 MOG PC-MR errors in pump frequency and maximum–minimum velocity (columns) for each pump setting sorted according to declining timer and beaker flow (rows)

	MOG Pump Frequency Error (bpm)	MOG Maximum–Minimum Velocity Error (%)	MOG Maximum–Minimum Velocity Error (cm/s)
Pump program 1 Timer and beaker flow: 701 mL/min Gated PC-MR VNR: 6.0 Gated PC-MR SNR: 55.2	2.4	−9.8	−14.1
Pump program 2 Timer and beaker flow: 452 mL/min Gated PC-MR VNR: 5.0 Gated PC-MR SNR: 53.9	−2.3	−5.6	−7.1
Pump program 3 Timer and beaker flow: 253 mL/min Gated PC-MR VNR: 3.7 Gated PC-MR SNR: 53.0	−16.0	−51.9	−50.6
Pump program 4 Timer and beaker flow: 127 mL/min Gated PC-MR VNR: 2.4 Gated PC-MR SNR: 47.0	−15.6	−53.4	−36.6

The 2 pump programs with low timer and beaker flow have larger MOG errors in both pump frequency and maximum–minimum velocity compared to the 2 pump settings with high timer and beaker flow.

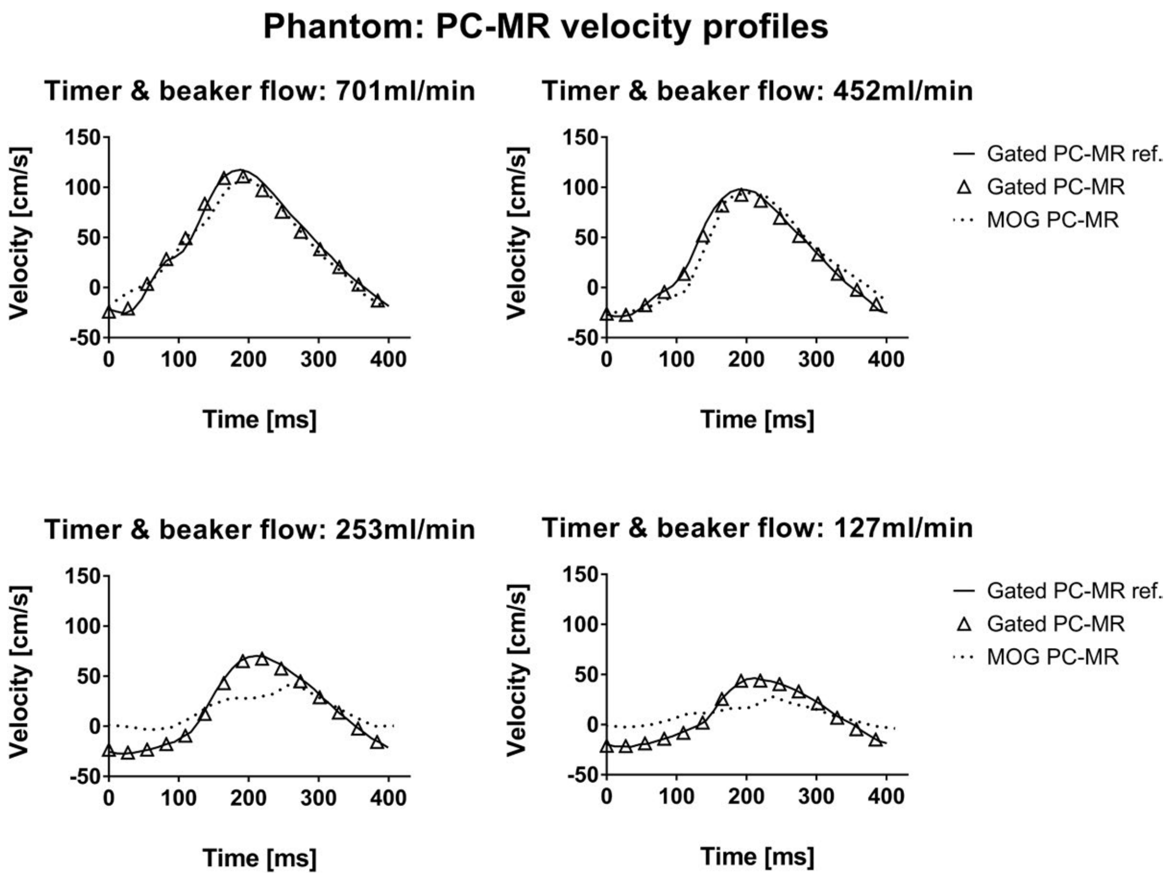

FIGURE 1 In the phantom experiment, MOG PC-MR underestimated maximum–minimum velocity at pump settings with low flow (bottom panels). The 4 panels show velocity profiles from the 3 evaluated PC-MR sequences (Table 1) at 4 pump settings with different flow. For the 2 pump settings with largest flow (top panels), MOG PC-MR (dotted lines) and the gated PC-MR sequence with similar acquisition parameters as MOG PC-MR (open triangles) were both in good agreement with the gated PC-MR velocity reference standard sequence (solid lines), whereas MOG PC-MR underestimated velocity peaks at the 2 pump settings with low flow (bottom panels). MOG PC-MR, metric optimized gating phase-contrast MR.

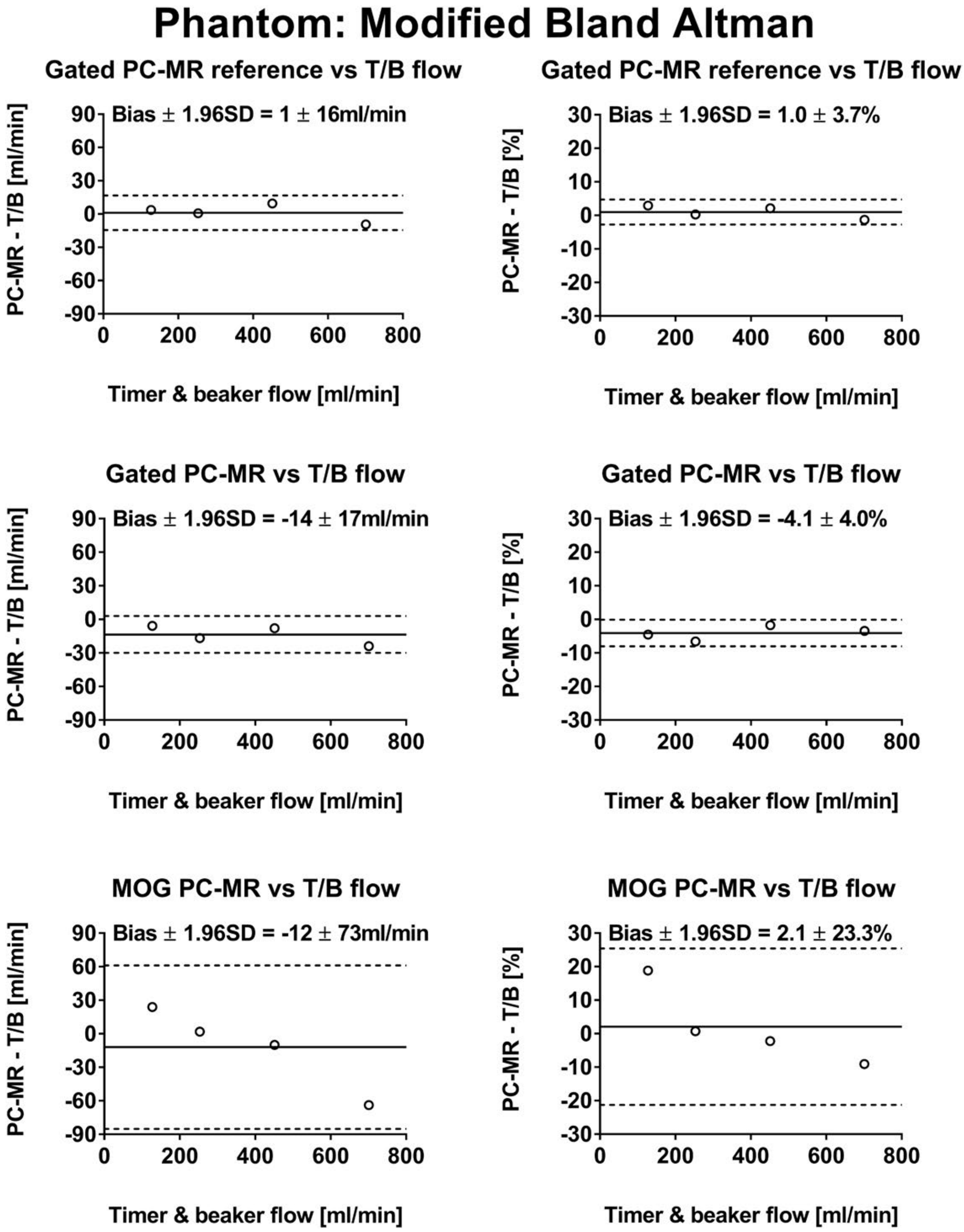

FIGURE 2 Metric optimized gating PC-MR shows low flow bias and high flow variability (bottom panels). The panels show modified Bland Altman analysis comparing PC-MR flow measurements with T/B flow in absolute volumes (left panels) and percentage units (right panels). Open circles indicate individual data points; solid lines indicate bias and dashed lines indicate bias ± 1.96 SD. The gated PC-MR velocity reference standard sequence (top panels) showed good agreement with T/B flow with low bias and variability. The gated PC-MR sequence with similar acquisition parameters as MOG PC-MR (middle panels) also demonstrated low bias and variability, whereas MOG PC-MR (bottom panels) resulted in increased flow variability compared to both conventionally gated PC-MR sequences (top and middle panels). T/B, timer and beaker.

flow before and after PC-MR measurements was less than 13.1 mL/min (1.86%), indicating stability of the flow reference standard measurement and low pump stroke volume variation.

3.1.1 | Gated PC-MR velocity reference standard measurements

The maximum flow difference between the gated PC-MR velocity reference standard sequence and timer and beaker was 9.6 mL/min (2.9%), suggesting good agreement between gated PC-MR flow and timer and beaker flow. Maximum–minimum velocities for all pump programs ranged between 68 to 143 cm/s.

3.1.2 | Gated PC-MR matched sequence measurements

Maximum flow differences compared to timer and beaker increased using the gated PC-MR sequence with sequence parameters similar to the MOG acquisition (−23.9 mL/min and −6.6%). Maximum–minimum velocity bias and variability compared to the gated PC-MR velocity reference standard sequence was −4 ± 2 cm/s (−3.7% ± 1.1%), indicating good agreement with the velocity reference standard.

3.1.3 | MOG PC-MR measurements

Estimated pump frequency from MOG reconstructions ranged from 130 to 150 bpm and resulted in error ranges −16 to −2.4 bpm compared to the true pump frequency (Table 2, rows 2 and 4).

Velocity profiles from MOG PC-MR and gated PC-MR sequences are shown in Figure 1. MOG PC-MR velocity profiles closely resembled gated PC-MR velocity profiles, except for the 2 pump settings with low flow and velocity. At all pump settings, MOG PC-MR underestimated maximum–minimum velocity compared to the gated PC-MR sequence with similar acquisition settings, with bias and variability −23 ± 42 cm/s (−27.5% ± 53.0%). Figure 2 shows a comparison between PC-MR and timer and beaker flow. MOG PC-MR overestimated flow at the pump setting with minimum timer and beaker flow (18.8%) and underestimated flow at the pump setting with maximum timer and beaker flow (−9.1%). Maximum difference in flow between MOG PC-MR and timer and beaker was −63.8 mL/min and 18.8%.

Low errors in estimated pump frequency and maximum–minimum velocity from MOG were found for the 2 pump settings (Table 2, rows 2–3) with VNR between 5 through 6. For the 2 remaining pump settings (Table 2, rows 4–5) with lower VNR (2.4 to 3.7), errors in estimated pump frequency and maximum–minimum velocity increased.

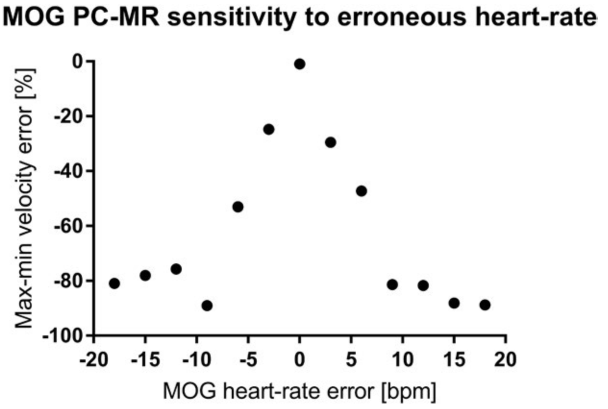

FIGURE 3 In the phantom experiment, MOG PC-MR maximum–minimum velocity measurements were sensitive to heart rate errors from MOG reconstruction (*x*-axis). The *y*-axis shows the error in the maximum–minimum velocity from MOG PC-MR compared to gated PC-MR for the pump setting with largest VNR. In the phantom experiment, a heart rate error less than approximately 3 bpm was required to achieve a maximum–minimum velocity error below 30%. bpm, beats per minute; VNR, velocity-to-noise ratio.

To investigate the underlying cause of the 2 outlier cases (Table 2, rows 4–5), new MOG reconstructions were performed using different reconstruction settings for increased noise robustness. A constant heart rate was assumed with a search step of 2 bpm, and the MOG ROI width was reduced from 11 to 3 pixels, covering only the phantom outflow nozzle. The new MOG reconstructed velocity profiles are shown in Supporting Information Figure S1. For the pump program with timer and beaker flow 253 mL/min, the new reconstruction matched the reference velocity profile. The pump frequency error was reduced from −16 bpm to −5.8 bpm, and maximum–minimum velocity error was reduced from −51.9% to −5.4%. For the pump program with timer and beaker flow 127 mL/min, the new MOG reconstruction did not resemble the reference velocity profile, and the maximum–minimum velocity error from MOG remained large (−46.8%). Supporting Information Animations S1 through S6 show PC-MR images after MOG reconstruction at all pump settings.

Figure 3 shows the relationship between errors in MOG heart rate estimation and errors in MOG PC-MR maximum–minimum velocity, indicating that a MOG heart rate error less than approximately 3 bpm was required to achieve a maximum–minimum velocity error lower than 30%. Results from numerical experiments are shown in Supporting Information Text S2 and Supporting Information Table S1.

3.2 | Fetal imaging

Supporting Information Figure S2 shows an example of a fetal MOG PC-MR flow measurement. One umbilical vein case was excluded due to major fetal movement. For interobserver variability, 2 other umbilical vein cases were not delineated by observer 2 due to challenging image quality and were excluded from interobserver analysis. Diameters for the fetal descending aorta and umbilical vein ranged between 5 to 8 mm and 5 to 9 mm, respectively. Pulsatility was shown for DAo but not for UV after MOG reconstruction in all subjects. Flow ranged between 546 and 948 mL/min in DAo and 181 to 606 mL/min in the UV. Intra- and interobserver variability were for DAo 7 ± 83 mL/min (bias ± 1.96 SD) and 55 ± 263 mL/min, and for UV 9 ± 70 mL/min and 56 ± 115 mL/min, respectively (Supporting Information Figure S3). Intra- and interobserver coefficient of variation for DAo were 6% and 19% and for UV were 10% and 17%. Noise SDs were for DAo 7.5 ± 3.1 cm/s (mean ± SD) and for UV were 9.6 ± 3.4 cm/s.

4 | DISCUSSION

This study presents phantom validation of the MOG method for a range of flow values similar to the fetal descending aorta and umbilical vein, together with inter- and intraobserver variability for fetal MOG PC-MR measurements. Low bias was found for MOG PC-MR flow measurements in phantom experiments, although velocities were underestimated for low VNR. Inter and intraobserver variability for MOG PC-MR imaging in vivo were comparable to previously reported values.[23]

Our phantom validation adds data compared to previous MOG validation studies[21,24] in 2 specific areas. First, phantom experiments in the current study included timer and beaker flow measurements as reference standard. Second, the flow phantom setup in the current study enabled validation for a range of flow velocities, a pump frequency, and a nozzle inner diameter similar to fetal vessels.

In the phantom experiment, MOG PC-MR underestimated flow at high flow values and overestimated flow at low flow values compared to timer and beaker. MOG PC-MR flow underestimation at high flow probably originates from the observed underestimation of velocity peaks; however, the MOG PC-MR flow overestimation at low flow may be caused by reduced flow pulsatility due to MOG misgating, leading to near constant and positive velocity over the RR interval.

Erroneous MOG PC-MR velocity profiles at low flow and velocity can likely be attributed to either limited VNR or the specific MOG reconstruction settings in use. The MOG reconstruction errors found at pump settings with low velocity partly originated from MOG reconstruction parameter settings because accurate velocity profiles were obtained at 1 of the outlier cases after re-tuning of MOG reconstruction settings. The initially selected 11 pixels wide ROI was larger than the tubing diameter, covering both areas with stationary and flowing water. The increased MOG accuracy using a reduced ROI for reconstruction is likely related to exclusion of regions containing stationary water, enhancing the pulsatile flow component in the ROI average. Of note, the performed tuning of reconstruction settings in the phantom validation is not a feasible option for in vivo fetal applications because the assumption of a constant heart rate is not realistic for fetal imaging. Numerical experiments demonstrated that VNR levels similar to those found for the 2 MOG outlier cases gave rise to errors in estimated heart rate in the same range as for errors observed in the phantom study, which is in line with our hypothesis.

Residual background phase error was likely not a major confounding factor in the phantom experiment because low bias and variability was found between timer and beaker flow and gated PC-MR flow.

The finding that MOG PC-MR is more sensitive to VNR compared to conventionally gated PC-MR should not discourage the use of MOG PC-MR in fetal MRI but rather warrants optimization of sequence parameters to each fetal vessel of interest. Further work is needed to determine which specific sequence parameter optimization is best suited for improving MOG reconstruction robustness.

For fetal imaging, flow volumes and intra- and interobserver variability in the fetal UV and DAo were comparable to previously reported values.[23] For analysis of MOG-reconstructed PC-MR images, the main source of variability is likely attributed to differences in vessel delineation. The interobserver variability, being slightly higher than intraobserver variability, indicates that delineation of fetal quantitative flow images poses additional challenges compared to corresponding analysis in children and adults. This may in part be related to lower image quality due to limited spatial resolution but also due to fetal movement and residual gating error after MOG reconstruction.

Velocity-to-noise regimes for in vivo fetal MOG PC-MR measurements were further analyzed because phantom validation showed MOG misgating at low VNR. In DAo and UV, VNR could not be directly determined because velocities were measured by the investigated MOG method in this study. However, noise SDs were estimated in acquired images without MOG processing from the current data set and combined with peak velocities in the corresponding vessels assessed in a previous study,[31] in which fetal PC-MR was gated using a doppler ultrasound device. The VNR regimes for the fetal DAo and UV were thus estimated to 8.0 and 1.6, respectively. These values were similar to VNR regimes in the current phantom validation, which resulted in both successful (DAo VNR = 8.0) and failed (UV VNR = 1.6) MOG reconstructions. The estimated VNR difference between DAo and UV further warrants sequence parameter optimization to individual fetal vessels and expected velocities for accurate MOG PC-MR.

4.1 | Limitations

Phantom studies did not include heart rate variability. However, this has been evaluated previously.[21]

The present study did not investigate the accuracy of background phase correction in fetal imaging, which may be challenging due to the lack of stationary tissue adjacent to the vessel of interest. Furthermore, the currently used PC-MR sequences for fetal flow measurements result in approximately 4 to 5 pixels across the vessel lumen of the intraabdominal umbilical vein and the fetal descending aorta during the third trimester. Although considered sufficient for accurate PC-MR velocity measurements,[16] limited spatial resolution may cause bias in flow measurements due to partial volume effects influencing ROI delineation.

Cardiotocography was not performed in all fetuses. However, the simulated RR interval of 525 ms used for MOG PC-MR corresponds to a fetal heart rate of 115 bpm, which is lower than expected in healthy fetuses.

5 | CONCLUSION

Phantom validation showed good agreement between MOG and conventionally gated PC-MR, except for cases with low VNR, which resulted in MOG misgating and underestimated peak velocities, which warrants optimization of sequence parameters to individual fetal vessels. Inter- and intraobserver variability for fetal MOG PC-MR imaging were comparable to previously reported values.

ORCID

Johannes Töger http://orcid.org/0000-0002-3365-7282
Anthony H. Aletras http://orcid.org/0000-0002-3786-3817

REFERENCES

1. Gill RW. Pulsed Doppler with B-mode imaging for quantitative blood flow measurement. *Ultrasound Med Biol.* 1979;5:223-235.
2. Eik-Nes SH, Brubakk AO, Ulstein M. Measurement of human fetal blood flow. *Br Med J.* 1980;280:283-284.
3. Thuring A, Laurini R, Maršál K. Uterine venous blood flow in normal and complicated pregnancies: A methodological study. *Ultrasound Obstet Gynecol.* 2010;35:462-467.
4. Gill RW. Measurement of blood flow by ultrasound: accuracy and sources of error. *Ultrasound Med Biol.* 1985;11:625-641.
5. Baker P, Johnson I, Harvey P, Gowland P, Mansfield P. A three-year follow-up of children imaged in utero with echo-planar magnetic resonance. *Am J Obstet Gynecol.* 1994;170:32-33.
6. Myers C, Duncan K, Gowland P, Johnson I, Baker P. Failure to detect intrauterine growth restriction following in utero exposure to MRI. *Br J Radiol.* 1998;71:549-551.
7. Schenck J. Safety of strong, static magnetic fields. *JMagn Reson Imaging.* 2000;12:2-19.
8. Clements H, Duncan K, Fielding K, Gowland P, Johnson I, Baker P. Infants exposed to MRI in utero have a normal paediatric assessment at 9 months of age. *Br J Radiol* 2000;73:190-194.
9. Kok R, de Vries M, Heerschap A, van den Berg P. Absence of harmful effects of magnetic resonance exposure at 1.5 T in utero during the third trimester of pregnancy: a follow-up study. *Magn Reson Imaging.* 2004;22:851-854.
10. Beerbaum P, Körperich H, Gieseke J, Barth P, Peuster M, Meyer H. Blood flow quantification in adults by phase-contrast MRI combined with sense: a validation study. *JCardiovasc Magn Reson.* 2005;7:361-369.
11. Lotz J, Döker R, Noeske R, et al. In vitro validation of phase-contrast flow measurements at 3 T in comparison to 1.5 T: precision, accuracy, and signal-to-noise ratios. *JMagn Reson Imaging.* 2005;21:604-610.
12. Gatehouse P, Rolf M, Graves M, et al. Flow measurement by cardiovascular magnetic resonance: a multi-centre multi-vendor study of background phase offset errors that can compromise the accuracy of derived regurgitant or shunt flow measurements. *JCardiovasc Magn Reson.* 2010;12:5.
13. Arheden H, Holmqvist C, Thilen U, et al. Left-to-right cardiac shunts: comparison of measurements obtained with MR velocity mapping and with radionuclide angiography. *Radiology.* 1999;211:453-458.
14. Carlsson M, Andersson R, Bloch K, et al. Cardiac output and cardiac index measured with cardiovascular magnetic resonance in healthy subjects, elite athletes and patients with congestive heart failure. *JCardiovasc Magn Reson.* 2012;14:51.
15. Rolf M, Hofman M, Gatehouse, PD et al. Sequence optimization to reduce velocity offsets in cardiovascular magnetic resonance volume flow quantification: a multi-vendor study. *JCardiovasc Magn Reson.* 2011;13:18.
16. Arheden H, Saeed M, Törnqvist E, et al. Accuracy of segmented MR velocity mapping to measure small vessel pulsatile flow in a phantom simulating cardiac motion. *JMagn Reson Imaging.* 2001;13:722-728.
17. Keegan J, Firmin D, Gatehouse P, Longmore D. The application of breath hold phase velocity mapping techniques to the measurement of coronary artery blood flow velocity: phantom data and initial in vivo results. *Magn Reson Med.* 1994;31:526-536.
18. Hofman M, Visser F, van Rossum A, Vink Q, Sprenger M, Westerhof N. In vivo validation of magnetic resonance blood volume flow measurements with limited spatial resolution in small vessels. *Magn Reson Med.* 1995;33:778-784.
19. Lund G, Wendland M, Shimakawa A, et al. Coronary sinus flow measurement by means of velocity-encoded cine MR imaging: validation by using flow probes in dogs. *Radiology.* 2000;217:487-493.
20. Bloch K, Carlsson M, Arheden H, Ståhlberg F. Quantifying coronary sinus flow and global LV perfusion at 3T. *BMC Med Imaging.* 2009;9:9.
21. Jansz M, Seed M, van Amerom J, et al. Metric optimized gating for fetal cardiac MRI. *Magn Reson Med.* 2010;64:1304-1314.
22. Tsai-Goodman B, Zhu M, Al-Rujaib M, Seed M, Macgowan C. Foetal blood flow measured using phase contrast cardiovascular magnetic resonance--preliminary data comparing 1.5 T with 3.0 T. *JCardiovasc Magn Reson.* 2015;17:30.
23. Prsa M, Sun L, van Amerom J, et al. Reference ranges of blood flow in the major vessels of the normal human fetal circulation

at term by phase-contrast magnetic resonance imaging. *Circ Cardiovasc Imaging*. 2014;7:663-670.
24. Seed M, van Amerom J, Yoo S, et al. Feasibility of quantification of the distribution of blood flow in the normal human fetal circulation using CMR: a cross-sectional study. *JCardiovasc Magn Reson*. 2012;14:79.
25. Heiberg E, Sjögren J, Ugander M, Carlsson M, Engblom H, Arheden H. Design and validation of Segment—freely available software for cardiovascular image analysis. *BMC Med Imaging*. 2010;11:10.
26. Töger J, Bidhult S, Revstedt J, Carlsson M, Arheden H, Heiberg E. Independent validation of four-dimensional flow MR velocities and vortex ring volume using particle imaging velocimetry and planar laser-Induced fluorescence. *Magn Reson Med*. 2015;75:1064-1075.
27. Tonge H, Struijk P, Wladimiroff J. Blood flow measurements in the fetal descending aorta: technique and clinics. *Clin Cardiol*. 1984;7:323-329.
28. Mahony B, McGahan J, Nyberg D, Reisner D. Varix of the fetal intra-abdominal umbilical vein: comparison with normal. *JUltrasound Med*. 1992;11:73-76.
29. Robson PM, Grant AK, Madhuranthakam AJ, Lattanzi R, Sodickson DK, McKenzie CA. Universal approach to quantification of SNR and g-factor for parallel MRI. In Proceedings of the 15th Annual Meeting of ISMRM, Berlin, Germany, 2007. p. 1747.
30. Bland J, Altman D. Statistical methods for assessing agreement between two methods of clinical measurement. *Lancet*. 1986;1:307-310.
31. Hedström E, Steding-ehrenborg K, Bidhult S, Ruprecht C, Kording F, Aletras AH. Quantitative phase-contrast CMR of blood flow in fetal vessels gated by Doppler ultrasound: comparison with metric optimized gating. In Proceedings of the 26th Annual Meeting of ISMRM, Paris, France, 2018. p. 2944.

SUPPORTING INFORMATION

Additional supporting information may be found in the online version of this article.

FIGURE S1 In the phantom experiment, re-tuned MOG reconstruction settings resulted in accurate MOG velocity profiles in one out of two outlier cases (top panel). The figure shows metric optimized gating (MOG) velocity profiles for the outlier cases both before (dotted lines) and after (solid lines) re-tuning of MOG reconstruction settings, together with conventionally gated PC-MR velocity profiles (open triangles). The remaining erroneous MOG velocity profiles (bottom panel) are likely caused by limited peak velocity of the underlying flow relative to the PC-MR velocity encoding in use (150cm/s). The re-tuning of MOG parameters was performed to investigate the cause of obtained velocity errors from MOG and is not feasible for in vivo fetal applications.

FIGURE S2 Magnitude (A and D) and velocity-encoded (B and E) MOG PC-MR images and corresponding typical flow curves (C and F) for the fetal descending aorta (top row) and umbilical vein (bottom row) with the respective vessel delineated in blue.

FIGURE S3 Bland-Altman analyses of intra- (left panels) and inter-observer (right panels) variability for flow measurements in the fetal descending aorta (DAo; top panels) and umbilical vein (UV; bottom panels). The dotted lines indicate bias and the solid lines indicate bias±1.96SD.

ANIMATION S1-S2 MOG PC-MR magnitude (left panels) and phase difference (right panels) image time series from pump settings 701ml/min and 452ml/min in the phantom experiment resulted in accurate pulsatile flow and phase difference images without severe misgating artifacts after MOG reconstruction.

ANIMATION S3-S4 MOG PC-MR magnitude (left panels) and phase difference (right panels) image time series from pump settings 253ml/min and 127ml/min in the phantom experiment resulted in clearly visible misgating artifacts in phase difference images after MOG reconstruction, indicating inaccurate heart rate estimation from MOG.

ANIMATION S5 With the modified MOG reconstruction settings, MOG PC-MR magnitude (left panels) and phase difference (right panels) image time series from pump setting 253ml/min in the phantom experiment resulted in accurate pulsatile flow and phase difference images without severe misgating artifacts after MOG reconstruction.

ANIMATION S6 With the modified MOG reconstruction settings, MOG PC-MR magnitude (left panels) and phase difference (right panels) image time series from pump setting 127ml/min in the phantom experiment did not result in accurate pulsatile flow, indicating inaccurate heart rate estimation from MOG. However, only subtle misgating artifacts were visible in phase difference images, indicating that misgating artifacts alone may be insufficient for determining the accuracy of MOG reconstructions.

How to cite this article: Bidhult S, Töger J, Heiberg E, et al. Independent validation of metric optimized gating for fetal cardiovascular phase-contrast flow imaging. *Magn Reson Med*. 2019;81:495–503. https://doi.org/10.1002/mrm.27392